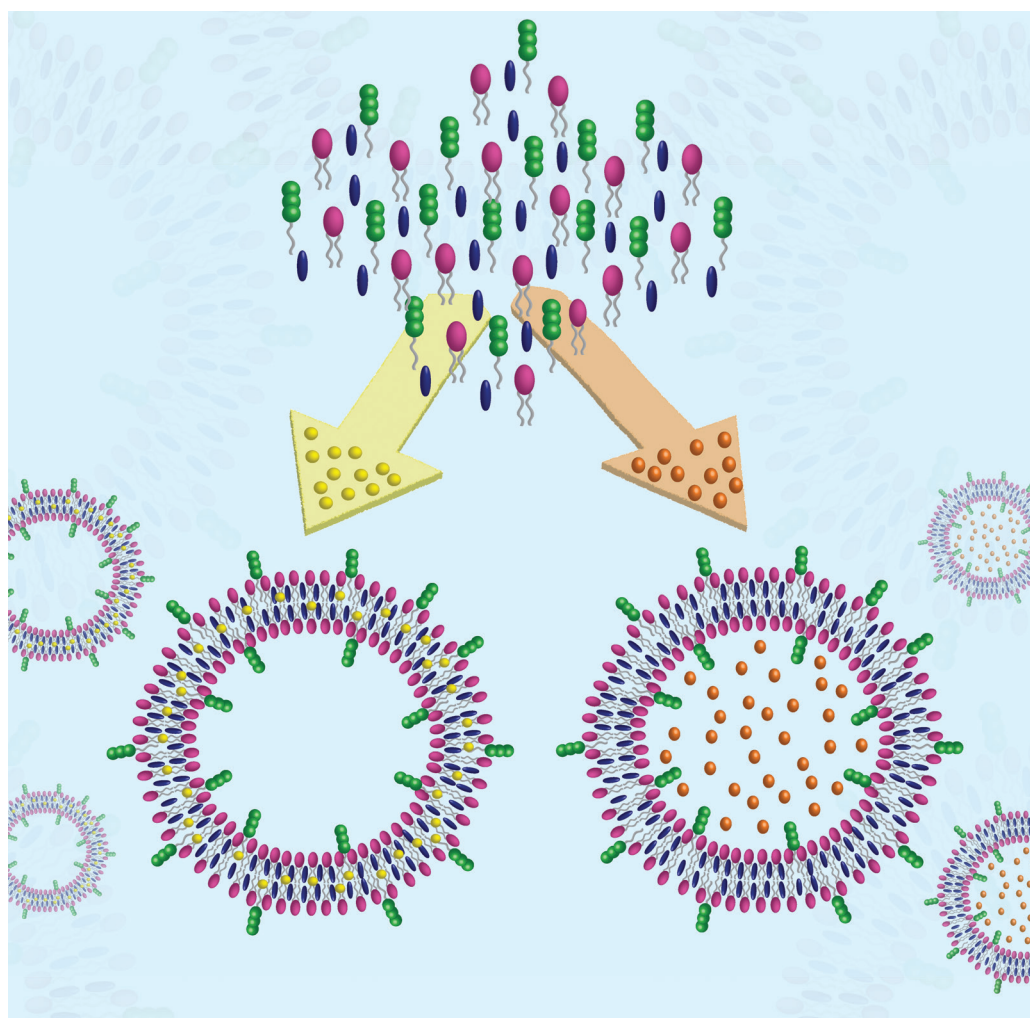


Self-Assembly of Biopolymers



PAPER

Cell penetrating peptide amphiphile integrated liposomal systems for enhanced delivery of anticancer drugs to tumor cells†

Melis Sardan,‡ Murat Kilinc,‡ Rukan Genc, Ayse B. Tekinay* and Mustafa O. Guler*

Received 24th April 2013, Accepted 24th June 2013

DOI: 10.1039/c3fd00058c

Liposomes have been extensively used as effective nanocarriers, providing better solubility, higher stability and slower release of drugs compared to free drug administration. They are also preferred due to their nontoxic nature as well as their biodegradability and cell membrane mimicking abilities. In this study, we examined noncovalent integration of a cell penetrating arginine-rich peptide amphiphile into a liposomal formulation of negatively charged 1,2-dioleoyl-*sn*-glycero-3-[phospho-*rac*-(1-glycerol)] (DOPG) phospholipids in the presence of cholesterol due to its amphipathic character. We studied changes in the physical characteristics (size, surface potential and membrane polarity) of the liposomal membrane, as well as in the encapsulation of hydrophilic and hydrophobic agents due to peptide amphiphile incorporation. The activities of peptide integrated liposomal systems as drug delivery agents were investigated by using anti-cancer drugs, doxorubicin-HCl and paclitaxel. Enhancement in liposomal uptake due to arginine-rich peptide integration, and enhanced efficacy of the drugs were observed with peptide functionalized liposomes compared to free drugs.

Introduction

Liposomes have been considered as potential drug delivery agents for several decades due to their biocompatibility, biodegradability and their resemblance to cell membrane.¹ Self-organization of lipid molecules into bilayer structures in aqueous environments through their amphipathic character results in the formation of spherical vesicles.² Their versatile nature enables the design of various functional liposomal systems decorated with a wide range of bioactive molecules such as antibodies, viral proteins, carbohydrates, peptides, aptamers,

Institute of Materials Science and Nanotechnology, National Nanotechnology Research Center (UNAM), Bilkent University, Ankara, Turkey. E-mail: moguler@unam.bilkent.edu.tr; atekinay@unam.bilkent.edu.tr; Fax: +90 312 266 4365; Tel: +90 312 290 3552

† Electronic Supplementary Information (ESI) available. See DOI: 10.1039/c3fd00058c

‡ These authors contributed equally.

and vitamins for therapeutic delivery.^{3,4} Various approaches have been used to functionalize liposomes including chemical coupling of the lipid molecules or ligand of interest before liposome formation, covalent conjugation of biologically active segments to the liposome surface and noncovalent association of liposome constituents.⁵⁻⁷

Amphiphilic peptides comprised of a bioactive peptide sequence and a hydrophobic segment have great potential for the functionalization of liposomal carriers. They can be designed and chemically synthesized with high yield and specificity and more importantly, they can be easily incorporated into liposomes noncovalently due to their lipid-like amphipathic properties with minimized activity loss or without laborious chemical functionalization steps.⁸⁻¹¹ The ease of functionalization together with their extensive encapsulation capacity make them attractive tools for the development of carrier systems, which can deliver cargo to the target with enhanced *in vivo* stability and circulation time.¹² Besides their facile integration, the versatility of peptide sequences provides diverse bio-functionality to the liposomal carriers.

The importance of cell penetrating peptides including HIV-Tat derived peptides, oligoarginines, and chimeric cell penetrating peptides has been emphasized in several studies for the delivery of therapeutic agents to target cells.^{13,14} Arginine-rich peptides have also been synthesized and investigated for enhanced cellular uptake efficiency by conjugation of fatty acids.¹⁵

Herein, we designed and synthesized an arginine-rich, cell penetrating peptide amphiphile molecule and examined its integration into a liposomal formulation of 1,2-dioleoyl-*sn*-glycero-3-[phospho-*rac*-(1-glycerol)] (DOPG) phospholipid in the presence of cholesterol. We studied the size, surface potential, and membrane polarity of the resulting liposomes with and without peptide amphiphile incorporation. Encapsulation capacities of these carriers were examined by using hydrophilic and hydrophobic dyes, rhodamine B and Nile red, respectively. After optimization of the encapsulation efficiencies of the liposomes, the *in vitro* uptake profiles and cytotoxicities of cancer drugs including doxorubicin-HCl and paclitaxel entrapped in liposomes with and without peptide amphiphile molecules were examined on the MCF7 human breast cancer cell line.

Experimental

Materials

9-Fluorenylmethoxycarbonyl (Fmoc) and *tert*-butoxycarbonyl (Boc) protected amino acids, [4-[α -(2',4'-dimethoxyphenyl) Fmoc-aminomethyl]phenoxy]acetamidonorleucyl-MBHA resin (Rink amide MBHA resin), and 2-(1*H*-benzotriazol-1-yl)-1,1,3,3 tetramethyluronium hexafluorophosphate (HBTU) were purchased from NovaBiochem and ABCR. Lauric acid was purchased from Merck. 1,2-dioleoyl-*sn*-glycero-3-[phospho-*rac*-(1-glycerol)] (DOPG) was purchased from Avanti Polar Lipids. Other chemicals were purchased from Alfa Aesar, Sigma-Aldrich or Applichem and used as provided.

Synthesis and characterization of peptide amphiphile molecule

The lauryl-PPPPRRRR-Am peptide amphiphile (PA) molecule was synthesized on MHBA Rink Amide resin. Amino acid couplings were performed with 2

equivalents of Fmoc protected amino acid, 1.95 equivalents of HBTU and 3 equivalents of *N,N*-diisopropylethylamine (DIEA) in DMF for 3 h. Fmoc removal was performed with 20% piperidine/dimethylformamide (DMF) solution for 20 min. Cleavage of the peptides from the resin was carried out with a mixture of trifluoroacetic acid (TFA) : triisopropylsilane (TIS) : water in the ratio 95 : 2.5 : 2.5 for 2 h. Excess TFA was removed by rotary evaporation. The remaining viscous peptide solution was treated with ice-cold diethyl ether and the resulting white pellet was freeze-dried. The peptide amphiphiles were identified and analysed by reverse phase HPLC on an Agilent 6530 accurate-Mass Q-TOF LC-MS equipped with an ESI source. An Agilent Zorbax SB-C8 4.6 mm × 100 mm column as the stationary phase and a water/acetonitrile gradient with 0.1% volume of formic acid as the mobile phase were used to identify peptide amphiphile molecules.

Liposome preparation

Liposomes were prepared *via* the curvature tuned preparation method reported previously.¹⁶ DOPG:Chol and PA integrated (DOPG:Chol:PA) liposomes were prepared with 1 : 1 and 7 : 8 : 1 molar ratios, respectively. Also, a DOPG:Chol:PA liposome with 7.5 : 8 : 0.5 formulation was prepared to evaluate the effect of peptide amphiphile density on the cellular uptake. For all liposomal formulations, 25 mg of total mixture was used. Samples were rehydrated in PBS buffer (10 mM, pH 7.4, 3% glycerol, with and without encapsulated material) at 65 °C under a nitrogen supply while the mixture was continuously stirred. The solution was treated with a rapid pH jump (pH 7.4 to pH 11 and to pH 7.4) carried out with an equilibrium period of 25 min, in which lipid clusters curled into encapsulating nanosized liposomes. The resulting liposomes were purified by using a G50 Sephadex column and stored at 4 °C.

Zeta-potential and dynamic light scattering measurements

The mean diameters and zeta-potentials of the liposomes were measured by using a Malvern ZetaSizer Nano-ZS ZEN 3600 (Malvern Instruments, USA) instrument with detector angle of 173°. Standard deviations were calculated from the mean of the data from a series of experiments ($n \geq 3$). Zeta potential measurements were carried out using a dip cell electrode in quartz cuvettes.

Transmission electron microscopy

Using a glass pipette, a drop of sample was placed on a 200 mesh formvar coated copper grid and carefully dried using filter paper. The sample was incubated at room temperature until a dried film was obtained. For PA free liposome, the sample was stained with 2 wt% phosphotungstic acid. Transmission electron microscope (TEM) imaging was performed by using a TEM (FEI Tecnai G2 F30) operated at 100 keV.

Quantification of the membrane integrated peptide amphiphile molecules

The protein concentration determination procedure provided by Thermo Scientific was utilized to measure the absorbance at 205 nm with an extinction coefficient of 31 mg mL⁻¹ at a 1 cm path length. The peptide amphiphile solutions were prepared in 0.6 mg mL⁻¹ concentrations. Free peptide amphiphile

molecules were removed by using Millipore Microcon Centrifugal Filter Units, with 50K MW cut-off. The retained sample was collected in each step and the peptide amphiphile concentration was measured by a Thermo Scientific Nano-Drop 2000 instrument. The amount of peptide amphiphile integrated into the liposomal membrane was then calculated by subtracting the amount of free PA from the initial PA concentration. This result was later used for calculation of the number of peptide amphiphiles per liposome.

Encapsulation capacities of liposomes

Rhodamine B was used as a model dye for hydrophilic molecules and encapsulated as described in the liposome preparation procedure. Free rhodamine B molecules were removed by using Millipore Microcon Centrifugal Filter Units, with 50K MW cut-off. The rhodamine B concentration was determined by fluorescence measurements ($\lambda_{\text{exc}} = 540 \text{ nm}$, $\lambda_{\text{em}} = 575 \text{ nm}$) following destruction of the liposome integrity by addition of ethanol (100 μL in 1900 μL ethanol). The total encapsulation efficiency was then calculated by $E (\%) = (\text{measured intensity} / \text{initial dye intensity}) \times 100$. Concentrations were calculated from a previously prepared standard curve. The same procedure was followed for a hydrophilic drug, doxorubicin-HCl, which was encapsulated with an initial concentration of 0.2 mg mL^{-1} . The standard curve was obtained by using the fluorescence intensity of doxorubicin-HCl ($\lambda_{\text{exc}} = 480 \text{ nm}$ and $\lambda_{\text{em}} = 588 \text{ nm}$).

Nile red was used as a model dye for hydrophobic drugs. A 1.5 mM Nile red stock solution was prepared in ethanol and further diluted in water to 0.01 mM. Nile red fluorescence intensity maxima switch with respect to the polarity of the environment and thus Nile red solubility in different types of liposomes was measured and compared in formulations of liposomes with and without peptide amphiphile molecules. The final concentration of 3 μM Nile red was introduced into the liposome dispersions by the addition of 450 μL of stock solution into 1.05 mL of diluted liposome (2.5 mg mL^{-1}) or PBS. The samples were left to equilibrate for 24 h at 4 °C before the measurements. The fluorescence intensity of liposomes in PBS ($\lambda_{\text{exc}} = 520 \text{ nm}$, $\lambda_{\text{em}} = 525\text{--}700 \text{ nm}$) was measured by a Varian Eclipse Fluorescence Spectrophotometer to determine the micellar character. The encapsulation of Nile red was studied by measuring the increased emission ($\lambda_{\text{exc}} = 476 \text{ nm}$, $\lambda_{\text{em}} = 633 \text{ nm}$) following the administration of 0.53 mM Nile red to previously prepared PA integrated and PA free liposomes. Liposomes were lysed by suspending 100 μL of sample in 1900 μL of ethanol and the amount of encapsulated Nile red was calculated by using a standard curve obtained using known concentrations of Nile red. For the hydrophobic drug model (paclitaxel), HPLC analysis optimized by Wang *et al.*¹⁷ was used to measure the encapsulation efficiencies of liposome formulations. Paclitaxel was extracted from the liposomes with acetonitrile (100 μL of liposome in 900 μL acetonitrile), then filtered with a 0.2 mm syringe filter and the concentration was analysed by using HPLC-1200S (Agilent). A 10 μL sample solution was injected into an Eclipse XDB-C18 (4.6 \times 150 mm, 5 μm) column. Water and acetonitrile (53 : 47) were used as the mobile phase. The elution rate was set to 1.0 mL min^{-1} and the paclitaxel detection wavelength was 229 nm. The number of integrated peptide amphiphiles and the amount of encapsulated material per liposome were calculated and the details of the related calculations can be found in the ESI.†

***In vitro* release of rhodamine B**

In vitro release of the hydrophilic rhodamine B from liposomes was studied in 10% FBS containing PBS medium.¹⁷ Rhodamine B encapsulated liposomes were placed in a dialysis bag (Spectra/Por membrane MWCO 500–1000 Da, 24 mm flat width, Spectrum Medical Industries, Los Angeles, CA) and released rhodamine B was collected in 50 mL PBS (pH 7.4 and pH 5.5) at 37 °C. 1 mL aliquots of dialysis solution were removed and replaced by equal volumes of fresh buffer solution at 37 °C. Rhodamine B release was measured by a Cary Eclipse fluorescence spectrophotometer for 72 h ($\lambda_{\text{exc}} = 540 \text{ nm}$, $\lambda_{\text{em}} = 575 \text{ nm}$).

Cytotoxicity studies

The cytotoxicity was evaluated by using the Alamar Blue™ assay. MCF7 cells were incubated in DMEM supplemented with 10% FBS and 1% penicillin/streptomycin under 5% CO₂ at 37 °C. Cells were cultured in a 96-well plate in 200 μL of medium per well with a density of 8×10^3 cells per well for 24 h. 50 μL of liposome with or without peptide formulation was administered with peptide concentrations of 250 μM , 25 μM and 12.5 μM ($n = 4$ for all groups). After 4 h and 24 h of treatment, the culture medium was replaced with serum free DMEM supplemented with 1% penicillin/streptomycin and 10% Alamar Blue™ solutions and the samples were incubated for an additional 4 h. Cell viability was quantified by measuring the fluorescence with excitation at 540 nm and emission at 590 nm with a microplate reader (Molecular Devices Spectramax M5).

***In vitro* uptake of peptide integrated liposomes**

MCF7 cells were seeded at a density of 3×10^4 cells per well in 24 well plates. 100 μL of liposome formulation was then administered and a 500 μL total culture volume was achieved. For rhodamine B loaded liposomes, administration was optimized to a final rhodamine B concentration of 4.5 μM . After 3 h of incubation, the culture medium was removed and the cells were washed two times with PBS. Then, the cells were lysed by using 100 μL of 0.5 M NaOH for 15 min with vigorous shaking in the dark. Lysates were collected and centrifuged at 15 000 rpm for 5 min. The rhodamine B concentration was measured from the supernatant by fluorescence measurements by a Nanodrop 3300 ($\lambda_{\text{exc}} = 540 \text{ nm}$, $\lambda_{\text{em}} = 590 \text{ nm}$). The fluorescence intensity was normalized to the protein concentrations of the total cell extracts in order to calculate the relative uptake. The protein concentration of the lysates was measured by the Bradford protein assay (Roche). In the case of Nile red loaded liposomes, the sample concentrations were adjusted to obtain 10 μM of final Nile red. After 3 h of incubation with Nile red loaded liposomes or free Nile red, the cells were washed as described above and lysed with 300 μL of 90 : 10 (v/v) ethanol : water for 15 min with vigorous shaking. Then, the lysates were centrifuged and fluorescence of the supernatant was measured ($\lambda_{\text{exc}} = 476 \text{ nm}$, $\lambda_{\text{em}} = 633 \text{ nm}$).

Fluorescence microscopy

MCF7 cells were seeded at a density of 1×10^4 cells per well in 24 well plates. 100 μL of sample solution was administered with Nile red at 10 μM . Following 24 h of incubation, the cells were washed two times with PBS and they were

directly mounted onto glass slides. 100 \times and 200 \times images were recorded by a Zeiss AxioCam™ fluorescence microscope. All imaging parameters were same for all of the experimental groups.

***In vitro* drug cytotoxicity: time and dose response**

The *in vitro* drug cytotoxicity of the doxorubicin-HCl and paclitaxel formulations were evaluated by using the Alamar Blue assay. MCF7 cells were cultured in 96-well plates at a cell density of 8×10^3 (for doxorubicin-HCl treatment) and 4×10^3 (for paclitaxel treatment) cells per well. Then, the cells were treated with drug loaded liposomes and free drug for another 24 h. After rinsing the cells with fresh media, the viability of the cells was quantified *via* the Alamar Blue assay. The cells were exposed to drug loaded liposomes or free drug for 1, 3 or 6 h, and the final drug concentrations were adjusted to 10 μ M for doxorubicin-HCl and 30 μ M for paclitaxel. Then, the cells were rinsed two times with fresh medium and incubated in standard cell culture medium for 24 h. Finally, the cytotoxicity levels and inhibition of cell proliferation were determined by the Alamar Blue assay.

Statistical analysis

All data are presented with the standard error of the mean (mean \pm SEM). One-way or two-way analysis of the variance (ANOVA) was used to determine the significance of differences between the groups. Differences are considered significant when $p < 0.05$.

Results and discussion

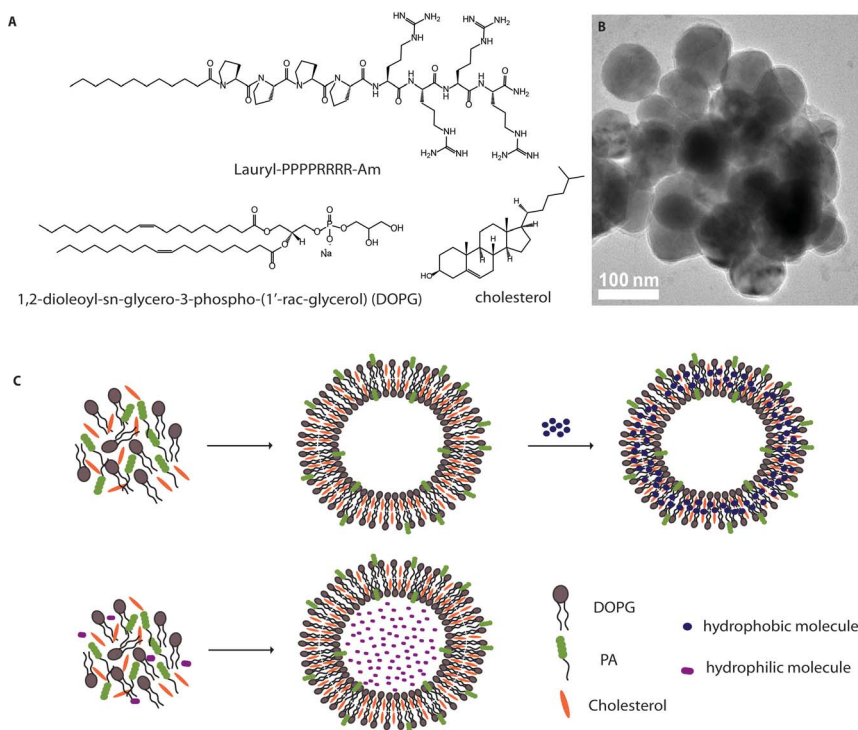
Synthesis and characterization of liposomes

Cell penetrating arginine-rich peptide amphiphile integrated and bare liposomes were prepared according to the curvature tuned liposome preparation (CTLP) method, where phospholipid residues are forced to be ordered in a nanostructure with the synergistic effect of a sudden pH jump and constant temperature.¹⁶ Addition of an amphiphilic molecule to the liposomal membrane can change the fluidity and curvature of the membrane, as well as the physical properties of the resulting liposome such as particle size, zeta potential and morphology. In this study, the negatively charged phospholipid DOPG was used as the main component of the liposomes.¹⁸ Previously, it was observed that DOPG liposomes prepared by the CTLP methodology with a size of 20 nm in diameter were not large enough to develop an efficient drug delivery system.¹⁹ Therefore, cholesterol was incorporated into the formulation to reduce the membrane curvature, which resulted in the formation of larger liposomes and provided intermediate membrane fluidity and prolonged circulation time.²⁰ As shown in Table S1,† we obtained uniform liposomes 63.5 ± 8.2 nm in diameter with a net negative charge of -41.4 ± 3.9 mV when the liposomes were formed by DOPG and cholesterol at a molar ratio of 50 : 50. Transmission electron microscopy images revealed that the resulting liposomes were unilamellar (Fig. S1†).

Liposome functionalization with cell penetrating peptides can be achieved by chemical conjugation of a peptide to the lipids before liposome preparation or directly to the liposome surface. Both strategies not only require additional steps and decrease the peptide integration efficiency but might also result in the loss of

biological activity.²¹ Therefore, developing noncovalent strategies is desirable to avoid chemical modifications.²² The use of amphiphilic peptides is a promising approach due to their resemblance to phospholipids.²³ Therefore, we designed and synthesized an arginine-rich peptide amphiphile molecule consisting of a lauryl group and arginine-rich peptide sequence, lauryl-PPPPRRRR-Am, (Scheme 1 and Fig. S2†). After peptide amphiphile integration, the particle sizes of the liposomes were measured to be 95.26 ± 7.03 nm and the membrane zeta-potential increased to -30.4 mV from -41.4 mV due to the positive net charge possessed by the peptide amphiphile molecule (Table S1 and Fig. S1†). The particle size of the liposomes stored at 4 °C was monitored, and no significant change was observed in the samples for over 3 weeks.

The amount of peptide molecules incorporated into the liposomal membrane was calculated by measuring the absorbance of the free peptide molecules collected during the purification process.²⁴ As shown in Table S1,† about four thousand peptide amphiphile molecules were estimated to be integrated per liposome. The peptide amphiphile insertion was also monitored by fluorescence assay by using Nile red as a polarity sensitive probe.²⁵ Nile red dispersion is usually colourless in aqueous conditions; however, changes in the environment of the hydrophobic dye revealed a switch from polar to nonpolar in the presence of



Scheme 1 (A) Chemical structures of peptide amphiphile (PA) lauryl-PPPPRRRR-Am, negatively charged phospholipid 1,2-dioleoyl-*sn*-glycero-3-phospho-(1'-*rac*-glycerol) (DOPG) and cholesterol. (B) Transmission electron microscopy image of PA integrated DOPG:Chol liposomes (scale bar = 100 nm). (C) Schematic representation for the preparation of PA integrated liposomes loaded with hydrophobic (Nile red, paclitaxel) or hydrophilic (rhodamine B, doxorubicin-HCl) molecules.

phospholipid and caused increased fluorescence emission. In the case of peptide-integrated liposomes, a blue shift was observed indicating a slight decrease in membrane polarity (Fig. S3†). The size and zeta-potential results also confirmed that peptide amphiphile molecules were embedded into the liposomal membrane, and increased the nonpolar character of the membrane, which can be considered as an advantage for the encapsulation of hydrophobic molecules.

Encapsulation of model reagents

Rhodamine B, a hydrophilic fluorescent dye, was used to probe the encapsulation capacities of liposomes prepared with and without peptide amphiphile molecules. Rhodamine B was administered during the liposome preparation and it was observed that the initial rhodamine B concentration affected the encapsulation capacities of the liposomes. Although the encapsulated dye concentration decreased slightly from 36.3 mM to 30.5 mM after PA integration, they encapsulated almost four times more rhodamine B compared to PA free liposomes due to their larger internal volume (Table S2†). To understand the effect of PA integration on the *in vitro* release of the entrapped rhodamine B, liposomes suspended in 10% FBS containing PBS medium were dialyzed at pH 5.5 and pH 7.4 against PBS at 37 °C. As shown in Fig. S4,† DOPG:Chol:PA liposomes were stable for over 72 h with no apparent release (<2%), while DOPG:Chol liposomes released 7.5% of the encapsulated rhodamine B. On the other hand, both liposome formulations released 17% of their content at pH 5.5. These results indicate that both formulations showed stability at both pH conditions and in serum containing PBS medium.

In addition, Nile red was used as a hydrophobic model molecule to observe the encapsulation capacities of PA integrated and bare liposomes. Since the hydrophobic dye encapsulation was performed after liposomes were prepared, free Nile red was first removed and encapsulated material was quantified by the calibration curve after destruction of liposomes in ethanol. Due to a slightly lower polarity and larger lipophilic surface area, PA integrated liposomes entrapped four times more Nile red with respect to the bare liposomes (Table S2†). The number of encapsulated dye molecules per liposome was found to be 7.9×10^5 and 3.13×10^6 for bare and PA integrated liposomes, respectively.

In vitro uptake of model dyes entrapped in liposomes

In order to evaluate the biocompatibility of liposomal formulations, MCF7 cells were treated with bare liposomes, PA integrated liposomes and PA molecules. Peptide amphiphile molecules did not cause significant change in cell viability in either the liposomal or free form after 4 h and 24 h of treatment (Fig. S5†). On the other hand, liposomal formulations had a positive effect on the cell proliferation after 24 h, which could be due to the use of liposomes as a nutritional source by cells.

The delivery efficiency of liposomes was evaluated by measuring the amount of fluorescent reagent taken up by MCF7 cells. Two dyes, hydrophilic rhodamine B and hydrophobic Nile red were separately used as model dyes. Tracking rhodamine B uptake is an efficient way to quantify liposomal uptake rates.^{26,27} Upon 3 h of treatment with equal amounts of rhodamine B, the use of PA integrated liposomes resulted in five times more rhodamine B uptake compared to

both native liposomes and free rhodamine B ($p < 0.001$) (Fig. 1). Although it was previously reported that the liposome size and their *in vitro* uptake rates are inversely proportional,²⁸ we observed that cell penetrating PA integrated liposomes, which are larger than bare liposomes, showed enhanced delivery of hydrophilic dye into the MCF7 cells. On the other hand, no significant difference was detected between the uptake of free rhodamine B and rhodamine B in bare liposomes. These results reveal that the noncovalent integration of cell penetrating PAs into liposomes improved cellular uptake of hydrophilic cargo by facilitating the liposome internalization. The cationic guanidine group of the arginine side chain has previously been shown to be important for the membrane translocation properties,²⁹ and might have enhanced the internalization of PA functionalized liposomes.

Several anticancer drugs including paclitaxel, cyclosporine, and amphotericin B have hydrophobic properties and are absorbed in the membrane of a liposome in addition to its lumen.³⁰ Nile red is a hydrophobic fluorescent dye and is therefore a suitable model molecule to track the behaviour of the lipophilic cargo in liposomes. MCF7 cells were treated with free Nile red, or Nile red encapsulated native or PA integrated liposomes for 3 h. The cells were imaged and cellular extracts were analysed by fluorescence spectroscopy. The fluorescence images indicated that DOPG:Chol liposomes facilitated the internalization of the hydrophobic cargo upon PA modification in contrast to unmodified liposomes (Fig. 2). Upon quantification of the relative uptake levels by Nile red extraction, PA integrated DOPG:Chol liposomes showed 30% increase in uptake ($p < 0.001$) compared to bare liposomes (Fig. 2). The uptake level of free Nile red was significantly lower than that of both PA modified and bare liposomes. Considering the number of Nile red molecules per liposome, a higher encapsulation capacity of PA integrated liposomes enables the administration of fewer liposomes compared to bare liposomes for delivering an equal concentration of Nile red (Table S2[†]). Therefore, our results suggest that PA integration enhances the hydrophobic Nile red uptake not only by increasing the encapsulation capacity of DOPG:Chol liposomes but also by enhancing liposome internalization.

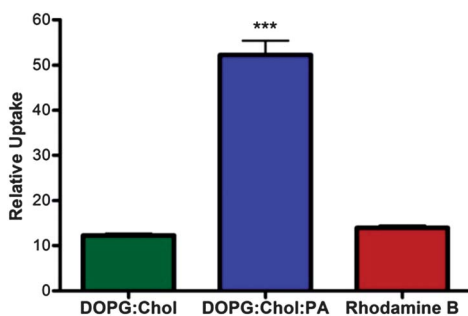


Fig. 1 Uptake of 4.5 μM rhodamine B within DOPG:Chol and DOPG:Chol:PA liposomes by MCF7 breast cancer cells after 3 h of treatment. Free rhodamine B was used as a control. The acquired signals were normalized to the protein concentration of the samples to calculate the relative uptake value. (***) stands for $p < 0.0001$ ($n = 4$).

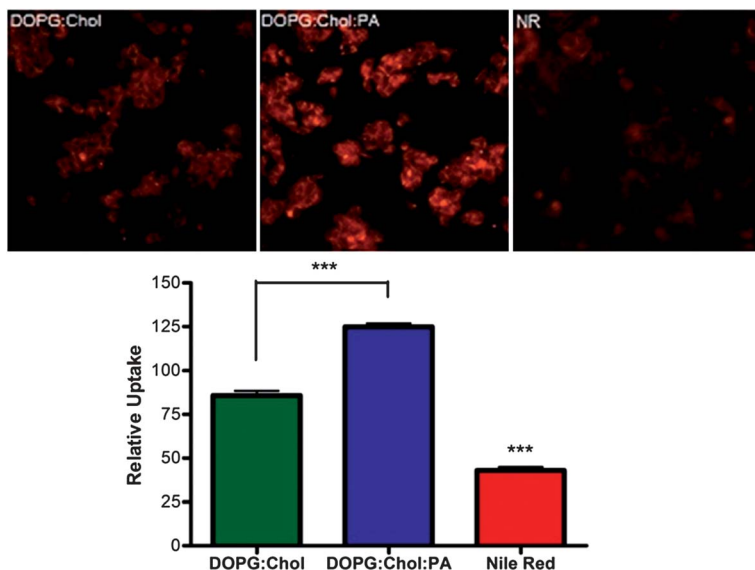


Fig. 2 Uptake of 10 μM Nile red by MCF7 cells. Nile red was administered in free or liposome encapsulated form for 3 h. Top: fluorescence microscopy images of cells following liposomal DOPG:Chol, DOPG:Chol:PA and free Nile red administration. Bottom: quantitative representation of Nile red taken up by tumor cells after 3 h of incubation. The acquired signals were normalized to the protein concentration of the samples. (***) stands for $p < 0.001$ ($n = 4$).

The effect of the amount of peptide incorporated into the liposomal system on the cellular uptake was also investigated by using a similar formulation (DOPG:Chol:PA) with less amount of peptide (7.5 : 8 : 0.5). The physical properties of the liposomes such as size and zeta potential were measured and the peptide amphiphile coverage and number of peptide amphiphiles per liposome were calculated (Table S3†). The amount of peptide did not significantly change the size and zeta potential of the liposome while the number of peptide amphiphile molecules integrated into one liposome decreased to 2706 from 4568. Liposomes containing less amount of PA exhibited similar encapsulation capacity to liposomes containing a higher amount of PA. The number of encapsulated Nile red molecules per liposome was found to be 3.04×10^6 . Upon quantification of the relative uptake levels by Nile red extraction, PA integrated DOPG:Chol liposomes demonstrated enhanced uptake compared to bare liposomes as the number of cell penetrating peptide amphiphile molecules increased (Fig. S6†). It has previously been demonstrated that the intracellular delivery of liposomes containing cell-penetrating peptides was enhanced with an increased number of peptide molecules attached onto the liposomes.^{31,32}

Encapsulation of doxorubicin-HCl and paclitaxel

The effect of arginine-rich cell penetrating peptide integration on liposomal delivery was investigated by using two well-known cancer drugs, hydrophilic doxorubicin-HCl and hydrophobic paclitaxel. For doxorubicin-HCl and paclitaxel encapsulation, 1 : 25 and 1 : 15 (w/w) liposomal content to drug ratios were used,

respectively. Both the liposome formulation and the liposome preparation methods are important parameters affecting the encapsulation capacity.^{33,34} Therefore, the effect of peptide integration on the amount of encapsulated doxorubicin-HCl was determined by using fluorescence spectroscopy, and paclitaxel carrying liposomes were analysed by HPLC to quantify the entrapment efficiency. The results are presented in Tables S4 and S5†. The native and PA integrated liposomes encapsulated 0.26 mM and 0.23 mM doxorubicin-HCl, respectively.

Paclitaxel is a known hydrophobic drug, which is currently used dissolved in a 50 : 50 (v/v) mixture of Cremophor® and ethanol. Drawbacks of current formulation, such as Cremophor® associated serious side effects and the possible precipitation of paclitaxel in aqueous media, require the development of new carrier systems with high encapsulation efficiency.³⁵ Similar to Nile red encapsulation results, PA integrated liposomes showed higher encapsulation efficiency for paclitaxel compared to bare liposomes. Less hydrophobic character of the PA integrated liposome membrane compared to bare liposomes might be the reason for enhanced encapsulation of paclitaxel. The concentration of encapsulated paclitaxel was found to be 92 μM in native liposomes and 117 μM in PA integrated liposomes (Table S5†). When the number of encapsulated molecules per liposome for each drug was calculated, the PA integrated liposomes showed superior encapsulation efficiency over bare liposomes (Tables S4 and S5†).

***In vitro* tumor inhibitory effect of native and PA integrated drug loaded liposomes**

The *in vitro* therapeutic effects of anticancer drug loaded PA integrated and PA free DOPG:Chol liposomes were evaluated *via* cytotoxicity assays and determination of cell proliferation rates by using the MCF7 breast cancer cell line. The activity of doxorubicin-HCl on tumor cells is mainly mediated by oxidative DNA damage and topoisomerase II inhibition in the nucleus, which results in apoptosis.³⁶ Here, the dose responses of doxorubicin-HCl loaded DOPG:Chol liposomes and free doxorubicin-HCl were evaluated by quantification of the total metabolic activity after 24 h of exposure (Fig. 3). Half maximal inhibitory concentration (IC_{50}) values were calculated as 2.58 μM , 2.48 μM and 0.88 μM for doxorubicin-HCl loaded DOPG:Chol, DOPG:Chol:PA liposomes and free drug (Fig. S7†). When used at low concentrations, liposomal doxorubicin-HCl has previously been shown to have lower toxicity compared to free doxorubicin.³⁷ The liposomal doxorubicin-HCl system is taken into the cell by endocytosis and is slowly released into the cytoplasm, which results in an increased number of barriers and slower therapeutic effect in contrast to free doxorubicin-HCl.^{24,37} These results show that increasing the concentration of doxorubicin-HCl enhanced the effectiveness of the liposome–doxorubicin-HCl systems.

Following dose response studies, the time dependent response of MCF7 cells to doxorubicin treatment was evaluated at 1, 3 and 6 h exposure times (Fig. 3). For the free and liposomal doxorubicin-HCl systems, the viability decreased with increasing exposure time. After 1 h of treatment, we observed that PA modified DOPG:Chol liposomes and free doxorubicin-HCl had almost two fold lower viability with respect to PA free DOPG:Chol liposomes ($p < 0.001$). The higher cytotoxicity of PA integrated liposomal doxorubicin-HCl demonstrated an

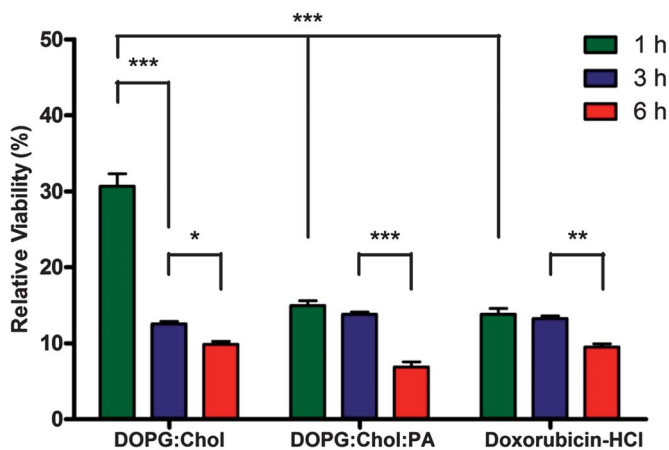


Fig. 3 Time response of MCF7 cells to 1, 3 and 6 h of 10 μM free or liposomal doxorubicin-HCl treatment. Following administration, cells were incubated in fresh media for further 24 h and the viability of the cells was measured. (***) stands for $p < 0.001$, ** stands for $p < 0.01$, * stands for $p < 0.05$) ($n = 4$).

improvement in the delivery efficiency caused by arginine-rich cell penetrating peptide incorporation into native liposomes. Bare liposomes exhibited a dramatic decrease in cell viability when the exposure time was increased from 1 h to 3 h ($p < 0.001$) while PA integrated liposomes and free doxorubicin-HCl did not show any significant difference. However, at 6 h of treatment, there was a significant decrease in cell viability for PA integrated liposomal doxorubicin-HCl and free doxorubicin-HCl ($p < 0.001$ for DOPG:Chol:PA and $p < 0.01$ for free doxorubicin-HCl) compared to shorter exposures. A statistically significant cell viability decrease was also observed for PA free liposomes ($p < 0.05$) after 6 h of drug exposure compared to shorter durations.

In addition, paclitaxel was used as a hydrophobic drug to examine the *in vitro* therapeutic effect of liposome encapsulated and free drug. Paclitaxel mainly acts as a G2/M cell cycle inhibitor and impedes cell proliferation by inhibiting microtubule dynamics.³⁸ We investigated the responses of MCF7 cells against free and liposomal paclitaxel in both time and dose dependent manners by determining cell proliferation inhibition. Dose dependent cytotoxicity studies demonstrated that PA integrated liposomes resulted in an enhanced therapeutic effect at all doses from 0.2 nM to 2 μM of paclitaxel ($p < 0.001$) compared to free paclitaxel (Fig. 4). As a result of 10 μM paclitaxel administration with DOPG:Chol and DOPG:Chol:PA, the viability of MCF7 cells was equally affected and decreased to about 50%. At this concentration, the inhibitory effect was two times higher for both PA integrated and native liposomes than that of free paclitaxel. The results reveal that both liposomes caused proliferation inhibition since the average doubling time of the MCF7 cells was 24 h and the number of untreated cells (control group) was doubled after 24 h.³⁹ These results show that enhanced cell growth inhibition *via* PA incorporated liposomes was observed for paclitaxel treatment with various concentrations. In addition, the response of MCF7 cells was evaluated by administering 30 μM of paclitaxel at 1 h, 3 h and 6 h. Both native and PA modified liposomes had time dependent cytotoxic response (Fig. 5). At

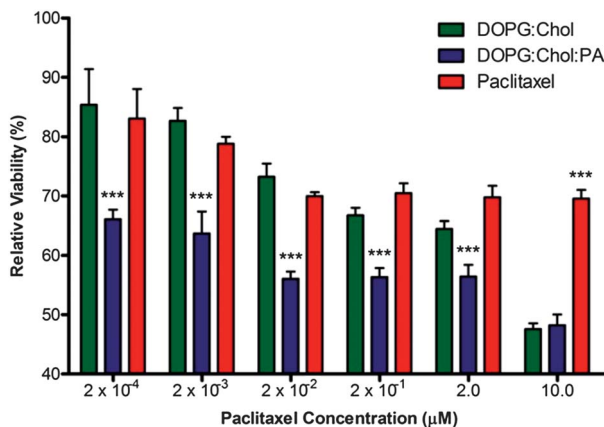


Fig. 4 Dose response of MCF7 cells against free paclitaxel and paclitaxel loaded DOPG:Chol and DOPG:Chol:PA liposomes within a spectrum of final concentrations ranging from 0.2 nM to 10 µM. After 24 h exposure to paclitaxel, the viability of the cells was measured. Cell proliferation in the presence of DOPG:Chol:PA liposomes was significantly lower ($p < 0.001$) than both DOPG:Chol liposomes and free paclitaxel at all paclitaxel concentrations except 10 µM. At 10 µM paclitaxel concentration, free paclitaxel showed a significantly lower effect compared to both DOPG:Chol and DOPG:Chol:PA liposomes ($p < 0.001$) ($n = 4$).

longer liposomal paclitaxel exposure, cell viability decreased by 25% in PA integrated liposomes while it did not change and remained at 75% in native liposomes. In the case of free paclitaxel, the therapeutic effect was not improved and the cell viability was close to that of native liposomes. Overall, our results suggest that PA integrated liposomes provide a more efficient delivery method for paclitaxel compared to PA-free liposomes and free drug.

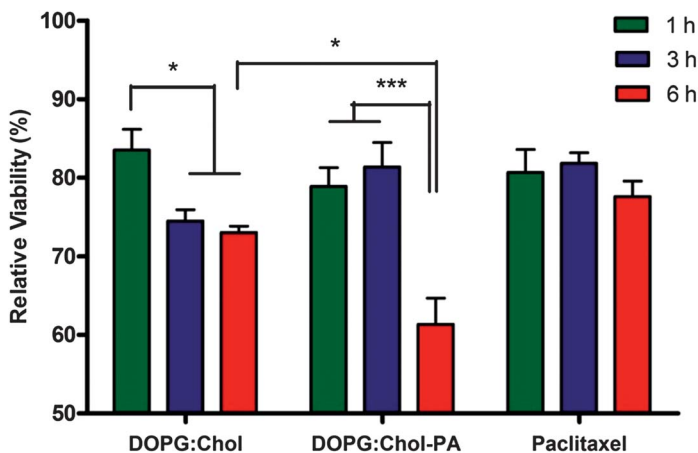


Fig. 5 Time response of MCF7 cells to 1, 3 and 6 h of 30 µM free or liposomal paclitaxel exposure. Cytotoxic effects of paclitaxel loaded DOPG:Chol and DOPG:Chol:PA liposomes. All results were normalized to the viability level of nontreated cells. (***) stands for $p < 0.001$, ** stands for $p < 0.01$, * stands for $p < 0.05$) ($n = 4$).

Conclusions

In summary, we developed a liposomal carrier system, which was decorated with cell penetrating arginine-rich peptide amphiphile molecules *via* the use of amphipathicity as an alternative functionalization method to chemical linkage. The resulting liposomes were found to be nontoxic and had high encapsulation capacity for both hydrophobic (Nile red) and hydrophilic (rhodamine B) model dyes with very slow *in vitro* release rates. Fluorescence measurements showed that the integration of the cell penetrating peptide amphiphiles to liposomes enhanced the uptake of model reagents by MCF7 breast cancer cells with respect to native liposomes as well as free reagents. The therapeutic effects of common cancer drugs, doxorubicin-HCl and paclitaxel, were studied *in vitro*. Cytotoxicity caused by the drug–liposome systems was observed to depend on the drug concentration. Time response studies showed that cell penetrating PA incorporation into DOPG:Chol liposomes improved liposomal delivery and enhanced the therapeutic effect of both hydrophilic (doxorubicin-HCl) and hydrophobic (paclitaxel) anticancer agents on MCF7 breast cancer cells. By use of this non-covalent functionalization technique, peptide epitopes can be easily incorporated into liposomal systems in one step without the need for any additional chemical reagents and the loss of activity is minimized by avoiding anchorage. Several peptide signals with different bioactive properties can be used to enhance the effectiveness of liposomal carriers, which have great potential in cancer treatment and imaging.

Acknowledgements

M. S. is supported by a TUBITAK-BIDEB PhD fellowship and R. G. is supported by a TUBITAK-BIDEB-2218 postdoctoral fellowship. We thank D. Mumcuoglu for help in the paclitaxel cytotoxicity experiments. M. O. G. and A. B. T. are partially supported by the Turkish Academy of Sciences Young Scientist Award (GEBIP).

References

- 1 R. J. Lee, *Mol. Cancer Ther.*, 2006, **5**, 1639–1640.
- 2 M. C. Woodle, *Adv. Drug Deliv. Rev.*, 1995, **16**, 249–265.
- 3 E. M. Rezler, D. R. Khan, J. Lauer-Fields, M. Cudic, D. Baronas-Lowell and G. B. Fields, *J. Am. Chem. Soc.*, 2007, **129**, 4961–4972.
- 4 V. Sihorkar and S. Vyas, *J. Pharm. Pharm. Sci.*, 2001, **4**, 138–158.
- 5 A. A. Kale and V. P. Torchilin, *Bioconjugate Chem.*, 2007, **18**, 363–370.
- 6 C. Yoshina-Ishii, G. P. Miller, M. L. Kraft, E. T. Kool and S. G. Boxer, *J. Am. Chem. Soc.*, 2005, **127**, 1356–1357.
- 7 D. W. Löwik, J. G. Linhardt, P. H. M. Adams and J. C. van Hest, *Org. Biomol. Chem.*, 2003, **1**, 1827–1829.
- 8 R. Tu, K. Mohanty and M. Tirrell, *Am. Pharm. Rev.*, 2004, **7**, 36–48.
- 9 Y.-C. Yu, V. Roontga, V. A. Daragan, K. H. Mayo, M. Tirrell and B. Gregg, *Biochemistry*, 1999, **38**, 1659–1668.
- 10 A. Garg, A. W. Tisdale, E. Haidari and E. Kokkoli, *Int. J. Pharm.*, 2009, **366**, 201–210.
- 11 G. D'Errico, A. M. D'Ursi and D. Marsh, *Biochemistry*, 2008, **47**, 5317–5327.
- 12 E. M. Rezler, D. R. Khan, R. Tu, M. Tirrell and G. B. Fields, *Methods Mol. Biol.*, 2007, **386**, 269–298.
- 13 E. Kokkoli, *Frontiers of Engineering: Reports on Leading-Edge Engineering from the 2010 Symposium*, 2011.
- 14 M. Magzoub and A. Graslund, *Q. Rev. Biophys.*, 2004, **37**, 147–195.
- 15 W. Pham, M. F. Kircher, R. Weissleder and C. H. Tung, *ChemBioChem*, 2004, **5**, 1148–1151.

- 16 R. Genc, M. Ortiz and C. K. O'Sullivan, *Langmuir*, 2009, **25**, 12604–12613.
- 17 F. Wang, Y. Chen, D. Zhang, Q. Zhang, D. Zheng, L. Hao, Y. Liu, C. Duan, L. Jia and G. Liu, *Int. J. Nanomed.*, 2012, **7**, 325–337.
- 18 N. Yanasarn, B. R. Sloat and Z. Cui, *Mol. Pharmaceutics*, 2011, **8**, 1174–1185.
- 19 R. Genc, G. Clergeaud, M. Ortiz and C. K. O'Sullivan, *Langmuir*, 2011, **27**, 10894–10900.
- 20 F. De Meyer and B. Smit, *Proc. Natl. Acad. Sci. U. S. A.*, 2009, **106**, 3654–3658.
- 21 M. Garcia, M. Alsina, F. Reig and I. Haro, *Vaccine*, 1999, **18**, 276–283.
- 22 S. Deshayes, K. Konate, G. Aldrian, L. Crombez, F. Heitz and G. Divita, *Biochim. Biophys. Acta, Biomembr.*, 2010, **1798**, 2304–2314.
- 23 F. Boato, R. M. Thomas, A. Ghasparian, A. Freund-Renard, K. Moehle and J. A. Robinson, *Angew. Chem.*, 2007, **119**, 9173–9176.
- 24 V. P. Torchilin, *Biopolymers*, 2008, **90**, 604–610.
- 25 E. Feitosa, F. R. Alves, A. Niemiec, M. E. C. R. Oliveira, E. M. Castanheira and A. L. Baptista, *Langmuir*, 2006, **22**, 3579–3585.
- 26 U. S. Huth, R. Schubert and R. Peschka-Süss, *J. Controlled Release*, 2006, **110**, 490–504.
- 27 R. Kikkeri, M. Maglino, P. Laurino, M. Collot, S. Y. Hong, B. Lepenies and P. H. Seeberger, *Org. Biomol. Chem.*, 2010, **8**, 4987–4996.
- 28 P. Machy and L. D. Leserman, *Biochim. Biophys. Acta, Biomembr.*, 1983, **730**, 313–320.
- 29 J. S. Lee and C.-H. Tung, *Mol. Biosyst.*, 2010, **6**, 2049–2055.
- 30 A. Sharma and U. S. Sharma, *Int. J. Pharm.*, 1997, **154**, 123–140.
- 31 V. P. Torchilin, *Adv. Drug Delivery Rev.*, 2008, **60**, 548–558.
- 32 Y.-L. Tseng, J.-J. Liu and R.-L. Hong, *Mol. Pharmacol.*, 2002, **62**, 864–872.
- 33 N. Duzgunes, *Liposomes*, Academic Press, 2004.
- 34 P. G. Tardi, N. L. Boman and P. R. Cullis, *J. Drug Targeting*, 1996, **4**, 129–140.
- 35 S.-J. Chung, C.-K. Shim and D.-D. Kim, *Int. J. Pharm.*, 2007, **338**, 317–326.
- 36 L. Pan, Q. He, J. Liu, Y. Chen, M. Ma, L. Zhang and J. Shi, *J. Am. Chem. Soc.*, 2012, **134**, 5722–5725.
- 37 S. Hussain, A. Plückthun, T. M. Allen and U. Zangemeister-Wittke, *Mol. Cancer Ther.*, 2007, **6**, 3019–3027.
- 38 S. Zhang, Q.-C. Zhang and S.-J. Jiang, *Chinese Med.*, 2013, **126**, 129–134.
- 39 R. L. Sutherland, R. E. Hall and I. W. Taylor, *Cancer Res.*, 1983, **43**, 3998–4006.